

Relation between molecular packing and singlet fission in thin films of brominated perylenediimides

Felter, Kevin M.; Dubey, Rajeev K.; Grozema, Ferdinand C.

DOI

[10.1063/1.5110306](https://doi.org/10.1063/1.5110306)

Publication date

2019

Document Version

Final published version

Published in

Journal of Chemical Physics

Citation (APA)

Felter, K. M., Dubey, R. K., & Grozema, F. C. (2019). Relation between molecular packing and singlet fission in thin films of brominated perylenediimides. *Journal of Chemical Physics*, 151(9), Article 094301. <https://doi.org/10.1063/1.5110306>

Important note

To cite this publication, please use the final published version (if applicable). Please check the document version above.

Copyright

Other than for strictly personal use, it is not permitted to download, forward or distribute the text or part of it, without the consent of the author(s) and/or copyright holder(s), unless the work is under an open content license such as Creative Commons.

Takedown policy

Please contact us and provide details if you believe this document breaches copyrights. We will remove access to the work immediately and investigate your claim.

Relation between molecular packing and singlet fission in thin films of brominated perylene-diimides

Cite as: J. Chem. Phys. **151**, 094301 (2019); <https://doi.org/10.1063/1.5110306>

Submitted: 15 May 2019 . Accepted: 11 August 2019 . Published Online: 03 September 2019

Kevin M. Felter , Rajeev K. Dubey , and Ferdinand C. Grozema 

COLLECTIONS

Paper published as part of the special topic on [Singlet Fission](#)

Note: This paper is part of the JCP special collection on Singlet Fission.



View Online



Export Citation



CrossMark

ARTICLES YOU MAY BE INTERESTED IN

[Method for real-time measurement of the nonlinear refractive index](#)

Journal of Applied Physics **126**, 093104 (2019); <https://doi.org/10.1063/1.5099220>

[Structural, band and electrical characterization of \$\beta\$ -\(Al_{0.19}Ga_{0.81}\)₂O₃ films grown by molecular beam epitaxy on Sn doped \$\beta\$ -Ga₂O₃ substrate](#)

Journal of Applied Physics **126**, 095702 (2019); <https://doi.org/10.1063/1.5113509>

[Visualizing carrier transitions between localization states in a InGaN yellow-green light-emitting-diode structure](#)

Journal of Applied Physics **126**, 095705 (2019); <https://doi.org/10.1063/1.5100989>

Lock-in Amplifiers up to 600 MHz

starting at

\$6,210



 Zurich
Instruments

Watch the Video 



Relation between molecular packing and singlet fission in thin films of brominated perylene diimides

Cite as: J. Chem. Phys. 151, 094301 (2019); doi: 10.1063/1.5110306

Submitted: 15 May 2019 • Accepted: 11 August 2019 •

Published Online: 3 September 2019



View Online



Export Citation



CrossMark

Kevin M. Felter,^{a)} Rajeev K. Dubey,^{a)} and Ferdinand C. Grozema^{b)}

AFFILIATIONS

Opto-Electronic Materials Section, Department of Chemical Engineering, Faculty of Applied Sciences, Delft University of Technology, Van der Maasweg 9, 2629 HS Delft, The Netherlands

Note: This paper is part of the JCP special collection on Singlet Fission.

^{a)}**Present address:** POLYMAT, Basque Center for Macromolecular Design and Engineering, Avenida de Tolosa 72, 20018 Donostia-San Sebastián, Spain.

^{b)}**Email:** F.C.Grozema@tudelft.nl

ABSTRACT

Perylene diimides (PDIs) are attractive chromophores that exhibit singlet exciton fission (SF) and have several advantages over traditional SF molecules such as tetracene and pentacene; however, their photophysical properties relating to SF have received only limited attention. In this study, we explore how introduction of bulky bromine atoms in the so-called bay-area PDIs, resulting in a nonplanar structure, affects the solid-state packing and efficiency of singlet fission. We found that changes in the molecular packing have a strong effect on the temperature dependent photoluminescence, expressed as an activation energy. These effects are explained in terms of excimer formation for PDIs without bay-area substitution, which competes with singlet fission. Introduction of bromine atoms in the bay-positions strongly disrupts the solid-state packing leading to strongly reduced excitonic interactions. Surprisingly, these relatively amorphous materials with weak electronic coupling exhibit stronger formation of triplet excited states by SF because the competing excimer formation is suppressed here.

Published under license by AIP Publishing. <https://doi.org/10.1063/1.5110306>

I. INTRODUCTION

Perylene diimides (see Fig. 1) are exceptionally photostable conjugated organic dye molecules that are attractive for application in optoelectronic devices such as solar cells. Apart from their strong electron accepting nature and their favorable charge transport properties, they have also been shown to exhibit singlet exciton fission (SF). SF is a spin-conserved process in which a singlet excited state shares its energy with a neighboring molecule to form a doubly excited state that consists of two coupled triplet excited states.¹⁻³ In addition, it has also been shown to undergo the inverse process, triplet-triplet annihilation up-conversion.⁴ SF is envisioned to be a viable approach to increase the power conversion efficiency of solar cells by using the excess energy in blue photons that is generally not used efficiently because of thermalization.⁵ In order to

fully exploit SF in photovoltaic applications, a fundamental understanding of the process is of prime importance. Specifically, as SF chromophores are generally applied in solid state devices, the relation between the dynamics of SF and the molecular packing and excited state energetics of the chromophores. The effect of molecular packing on singlet fission has been previously studied in acene chromophores. Theoretical⁶ and experimental results have been reported for tetracene,⁷ covalent dimers of pentacene⁸ in solution, and terylene diimides.⁹ The general conclusion from these studies is that SF rates and efficiencies can be optimized by optimizing the electronic coupling via the molecular organization in the solid state. Perylene diimides (PDIs) offer a unique opportunity to study the effect of molecular organization and energetics on singlet fission since variations in the substituents of the chromophore lead to changes in the solid state packing and excited state energetics. Computational

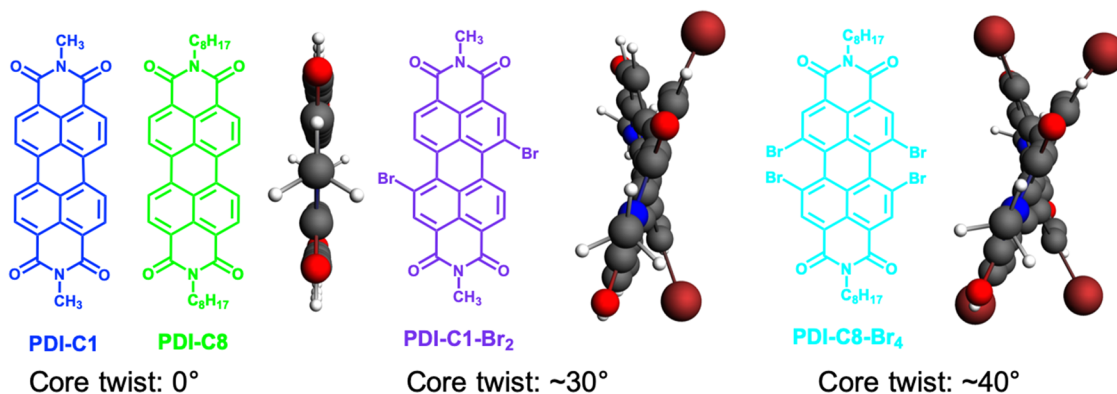


FIG. 1. Chemical structures of the perylene diimide molecules of interest in this study with different imide- and bay-substitution. The ball-and-stick structures display the twisted perylene core structure upon bromination in side view as is noted by the core twist.

and experimental studies have shown that changes in the molecular packing induced by imide-substituted PDIs indeed have a strong impact on the rate and efficiency of SF.^{3,10,11} While the effect of imide-substitution of PDIs on their optoelectronic properties has been studied widely owing to the relatively accessible synthesis, only few studies exist on the impact of substitution on the bay area, especially in relation to SF. It has been shown that PDIs substituted with halogens in the bay area (see Fig. 1) exhibit changes in the singlet and triplet state excited state energetics. This is due to the sterically induced twisting of the conjugated core of the PDI, as compared to their non-bay-area substituted analogs.^{12,13} Moreover, bay-area substitution leads to greatly improved solubility in common organic solvents, which is a desirable characteristic for eventual device applications.

In this study, we investigate how halogen substitution in the bay-area of PDIs affects the molecular packing and excitonic interactions in the solid state and how this affects the singlet fission dynamics in thin films of methyl (PDI-C1) and octyl (PDI-C8) imide-substituted PDIs. To achieve this, two or four bromide atoms have been introduced at the bay position of the PDI core as shown in Fig. 1. Steady state optical absorption and emission measurements on thin films revealed that bay-area bromination significantly reduces the excitonic interactions in the solid state. Nevertheless, from transient-absorption measurements, we clearly observe the formation of triplet excited states with efficiencies comparable to their unsubstituted analogs. This indicates that the reduced excitonic interaction does not prohibit SF. Furthermore, we have studied the temperature dependence of the optical absorption, emission, and photoluminescence (PL) lifetime. Only small differences in the optical absorption upon cooling were found, indicating a stable molecular arrangement. However, at the same time, strong increases in both PL intensity and lifetime were observed, proving the existence of a thermally activated PL competitive process. The detailed analysis of the effect of bay-area substitution on the excitonic interactions and SF dynamics presented in this work shows that bay area substitution offers an additional handle to tune the SF properties of PDI chromophores.

II. EXPERIMENTAL

A. Materials

The chemical structures of the PDI derivatives investigated in this work are shown in Fig. 1. PDI-C1 (*N,N'*-dimethyl-3,4,9,10-perylenedicarboximide) and PDI-C8 (*N,N'*-dioctyl-3,4,9,10-perylenedicarboximide) were synthesized from perylene-3,4,9,10-tetracarboxylic acid dianhydride as purchased from Sigma-Aldrich using procedures published elsewhere.¹⁴ PDI-PPh-Br₂ [*N,N'*-bis(2,6-diisopropylphenyl)-1,7-dibromo-perylene-3,4,9,10-tetracarboxybisimide], PDI-C1-Br₂, and PDI-C8-Br₄ were synthesized from 1,7-dibromoperylene dianhydride and 1,6,7,12-tetrabromoperylene dianhydride, respectively, as described in the [supplementary material](#).^{15,16} The powders of PDI-C1, PDI-C8, and PDI-C1-Br₂ were thermally evaporated (using an *AJA International* evaporator system) to make thin films on air plasma cleaned 1 × 2 cm² fused silica (also termed quartz) and sapphire substrates (from *Esco Optics*). The evaporated films were not annealed during or after deposition. Thin films of PDI-C8-Br₄ were spincoated from a saturated chloroform solution. The spincoated film was annealed at 60 °C in a N₂ atmosphere to remove any solvents and improve the crystallization. The film thicknesses were measured using a *Dektak profilometer* and are provided in Table S1 of the [supplementary material](#).

B. Methods

Temperature-dependent steady state absorption and emission spectra of the thin films were measured in a home-built He-cryostat spectroscopy setup. The sample is placed in a vacuum chamber (10⁻⁷ mbar) of which the temperature is controlled using an *APD-cryogenics* helium cryostat in the range 300–12 K. The optical absorption spectra were measured using the halogen lamp output of a *DH-200 Mikropack UV-VIS-NIR* light source and a *Maya2000 Pro* Ocean Optics spectrometer detector. The fluorescence emission spectra were measured using 3.15 mW (405 nm) laser pulses of a *CPS405 ThorLabs* laser diode and a *FLAME-S-VIS-NIR* Ocean

Optics spectrometer. Exposure of the sample to air was minimized by storing it in an N₂ glovebox and by flushing the sample chamber with N₂ during sample loading. Steady state absorption spectra of the thin films at room temperature were measured with a *Perkin Elmer Lambda 1050* spectrophotometer with the sample placed inside an integrating sphere to measure the attenuation.

Time-resolved photoluminescence measurements were performed with a *Lifespec-ps* fluorescence spectrophotometer (Edinburgh Instruments) using time-correlated single photon counting. The sample was photoexcited using 12.4 pJ (404 nm, 1 MHz) laser pulses from a *M8903-01 Hamamatsu* laser unit. In order to minimize laser scattering, a 425 nm long-pass filter was placed in front of the detector. The sample was loaded in an *Optistat DN cryostat* (Oxford Instruments) in an N₂ exchange gas environment. Excitation density effects were examined by placing a neutral density filter (optical density = 1) after the laser diode unit to exclude the presence of exciton-exciton annihilation. The thin film topology was measured using atomic force microscopy, and the crystallinity was studied using X-ray diffraction using a *Brüker D8* X-ray diffractometer (Co K α 1 radiation, $\lambda = 1.79$ Å) and analyzed with the Brüker program *EVA*.

Transient absorption measurements were performed using a *Helios* spectrometer (Ultrafast Systems) where the samples were excited with 180 fs pulses (2.5 kHz) from a *Pharos Yb:KGW* laser system (Light Conversion) via an *Orpheus* optical parametric amplifier (Light Conversion). The probe pulse consisted of supercontinuum light generated by focusing a part of the fundamental laser beam (1030 nm) in either a CaF₂ or sapphire crystal, depending on the required probe wavelength range. Nanosecond-time resolved emission and transient absorption spectra were acquired using an *LP920* transient absorption spectrophotometer (Edinburgh Instruments) with pulsed probe light (7 ns) produced by a Xe lamp. The samples were excited by 4 ns (FWHM) laser pulses produced by an *Ekspla NT 342B* optical parametric oscillator (OPO) pumped by a Q-switched Nd:YAG laser.

The effect of the bay-area substitution with Br atoms on the geometry and electronic structure was studied by density functional theory (DFT) and semiempirical calculations. The ground state geometries were optimized using the Becke-Perdew (BP86) exchange correlation (XC) functional with a double zeta polarized-type (DZP-type) basis set consisting of Slater-functions. Using this geometry, the vertical singlet and triplet excitation energies were calculated by TDDFT calculations in the same basis set and XC functional.

An approximate geometry for the lowest triplet state (the triplet ground state) was optimized by performing an open shell

triplet ground state calculation, using the BP86 functional with a DZP-type basis set. The absorption spectrum of this triplet ground state was calculated by an unrestricted TDDFT calculation. All calculations were done using the Amsterdam Density Functional software suite.

III. RESULTS AND DISCUSSION

To gain insight into the effect of bromination of the PDI core on the geometrical and basic photophysical properties, we have performed electronic structure calculations using Density Functional Theory (DFT) methods as described in Sec. II. The results are summarized in Table I. Ground state geometry optimizations show that bromination leads to a distinct deviation from the planar PDI geometry that is obtained without bromines attached. For PDI-Br₂, a twist angle of 29.2° was obtained, while for PDI-Br₄, an even larger twist angle of 39.1° was found. Twisting of the core is predicted to have a pronounced effect on the optical properties as can be derived from Table I. TDDFT calculations show that the energy difference between the ground state and the lowest singlet excited state S₁ decreases from 2.16 eV for the planar PDI-H₄, but decreases significantly to 2.01 eV and 1.95 eV for PDI-Br₂ and PDI-Br₄, respectively. Interestingly, the energy difference between the ground state and the lowest (vertical) triplet state remains almost unchanged upon bromination.

A. Effect of bromination on PDI optical properties

The attenuation and emission spectra of the different PDIs in solution and in the solid state are shown in Fig. 2. In solution, the absorption spectra of the PDIs with and without bromines exhibit the characteristic PDI S₀ → S₁ absorption with vibronic peaks at 475, 490, and 520 nm. Halogenation in the bay-area increases the absorption between 420 nm and 460 nm as a result of the symmetry forbidden S₀–S₂ transition for planar PDIs that becomes partially allowed in the strongly twisted PDI-C8-Br₄.^{12,17} The steady state emission spectra in solution display Stokes shifts of only a few nanometers for PDI-C1 and PDI-C8. The Stokes shift increases to almost 50 nm for PDI-C8-Br₄ indicating a larger excited state geometry relaxation.¹² In addition, the vibronic structure becomes less pronounced upon bromination as a result of the loss of the planarity of the PDI core and the broken symmetry.¹⁷ The impact of bay-area substitution on the molecular packing in the solid state can be observed by comparing the steady state absorption and emission spectra of the thin films with the respective solutions. A strong broadening and red-shift of the absorption features are observed for PDI-C1 and PDI-C8, reflecting close packing, accompanied by strong exci-

TABLE I. Summary of the calculated optical properties of bay area substituted PDIs using DFT.

PDI	Ground state			T ₁ state	
	Angle (deg)	E _{S1} (eV)	E _{T1} (eV)	Twist (deg)	T ₁ –T _n (nm)
PDI-H ₂	0	2.16	1.33	0	536 (2.31 eV)
PDI-Br ₂	29.2	2.01	1.33	22.3	566 (2.19 eV)
PDI-Br ₄	39.1	1.95	1.32	31.1	579 (2.14 eV)

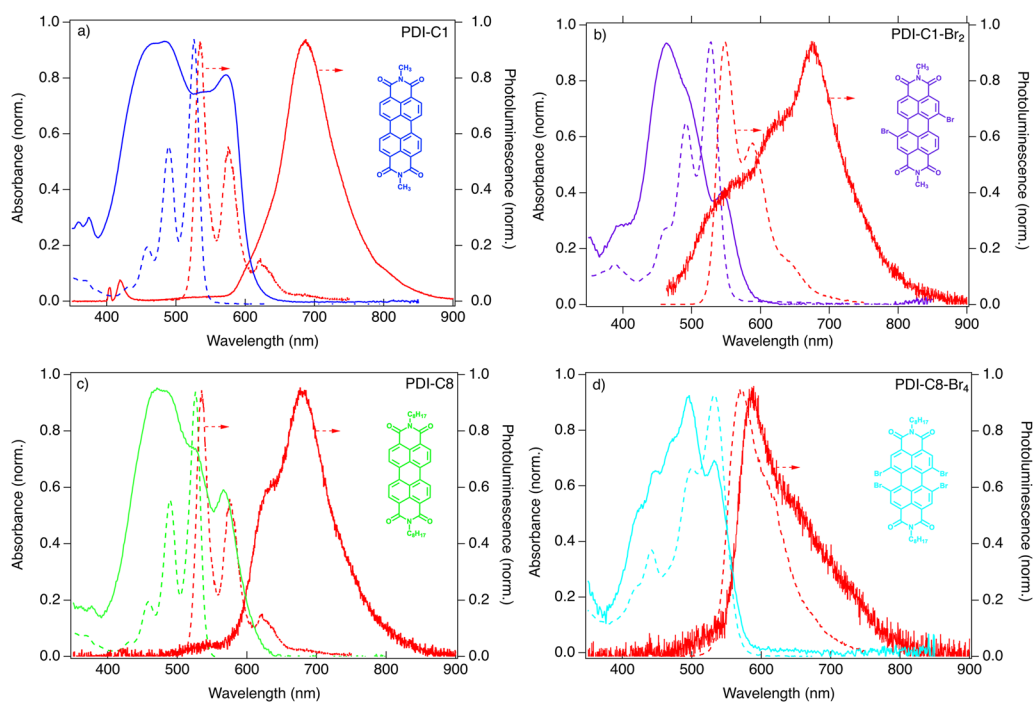


FIG. 2. Room temperature normalized steady state absorption and emission spectra for PDI-C1 (a), PDI-C1-Br₂ (b), PDI-C8 (c), and PDI-C8-Br₄ (d) thin films (solid lines). The solution spectra (dashed lines) shown in (a) and (c) come from dissolved PDI-C8 in chloroform, while for (b) and (d), PDI-PPh-Br₂ and PDI-C8-Br₄ dissolved in chloroform were used, respectively.

tonic coupling.¹⁸ For the brominated samples, these effects are much less pronounced. Similar to PDI-C1-Br₂, for PDI-C8-Br₄, there is a small reorganization of the molecules upon going from solution to the solid state, indicating weak crystal packing. Moreover, the emission spectra of PDI-C1 and PDI-C8 have a strong Stokes shift of 204 and 200 nm, respectively, which is typical of excimer emission.^{19–21} The reduced excitonic interactions can be traced back to lack of crystallization and hindered solid state packing in the brominated samples in comparison to PDI-C1 and PDI-C8 as substantiated by

the absence of reflections in X-ray diffractograms [Fig. S3(a) of the [supplementary material](#)] for PDI-C8-Br₄ thin films. However, the powders of all four PDIs show strong reflections, indicating the possibility to crystallize as shown in Fig. S3(b) of the [supplementary material](#).

As shown in Fig. 3(a), at 300 K the photoluminescence lifetimes in thin films (obtained from fitting the decay in the first 2 ns) vary from 700 ps for PDI-C1 to 890 ps for PDI-C8, which is typical of singlet exciton emission. These lifetimes are much shorter than

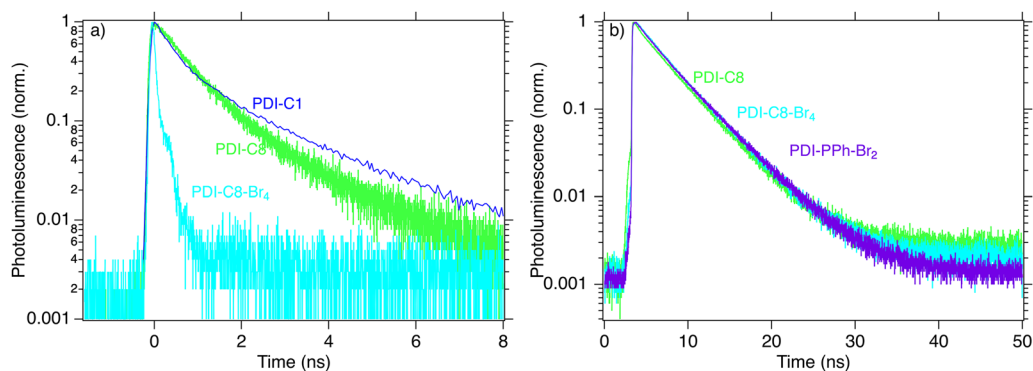


FIG. 3. Time-resolved PL spectra in thin films of PDI-C1, PDI-C8, and PDI-C8-Br₄ (a). In (b), the emission spectra in solution are shown for PDI-C8 (identical behavior for PDI-C1), PDI-PPh-Br₂ (identical behavior for PDI-C1-Br₂), and PDI-C8-Br₄.

for triplet excitons that typically have lifetimes of a few microseconds in PDI thin films.^{2,12} The fluorescence lifetimes in these solid films are considerably smaller than in chloroform solutions [$\tau = 4.5$ ns, Fig. 3(b)], indicating the presence of competing nonradiative decay processes in the solid. A possible cause of the reduced fluorescence lifetime due to closer packing, and thus enhanced electronic coupling between molecules in the solid state, is the occurrence of SF.¹⁻³ An alternative explanation is the formation of nonemissive excimer states. While intersystem crossing can be a third possible explanation for the reduced emission lifetime, this can be ruled out since the fluorescence lifetime of the PDIs in solution, shown in Fig. 3(b), is unaffected by bromination. This is consistent with previous studies.¹²

B. Effect of temperature on PDI thin film optical properties

In order to gain more insight into the excited state dynamics and decay pathways in these materials, we have performed temperature dependent optical absorption, emission, and time-resolved PL measurements at temperatures ranging from 300 K to 12 K. The temperature dependent steady state absorption spectra are shown in Fig. S4 of the [supplementary material](#). The changes in the optical absorption spectra of the thin films occurring upon cooling to liquid helium temperatures (12 K) are small. This indicates that the molecular packing is stable and no phase change occurs. In contrast, cooling results in significant changes in the emission spectra as shown in Fig. 4 in two ways. First, the emission intensity, and thus the fluorescence quantum yield, increases upon lowering the temperature, by two orders of magnitude in the case of PDI-C8. Second, the shape of the emission spectra changes, exhibiting stronger emission at higher energies. The narrowing of the emission band on the blue side may signify a weaker intermolecular interaction.¹⁸ Furthermore, at 93 K, the PL lifetime increases to 1.2 ns and 4.1 ns for PDI-C1 and PDI-C8, respectively, while the lifetime of the

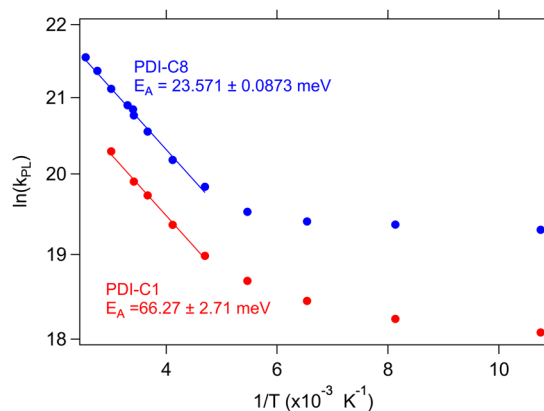


FIG. 5. Plot of the natural logarithm of the inverse fluorescence decay time of the different PDIs as a function of inverse temperature. The solid line represents the applied Arrhenius relation: $k_{PL} = Ae^{E_A/k_B T}$.

brominated PDIs is virtually unaffected upon decreasing the temperature as shown in Fig. S5 of the [supplementary material](#).

The increase in the PL quantum yield and lifetime are both indicative of an endothermic nonradiative decay pathway that outcompetes fluorescence at room temperature. The activation energies, E_A , for such an endothermic process have been obtained by plotting the natural logarithm of the photoluminescence decay rate, $\ln(k_{PL})$, as a function of the inverse temperature and by fitting the trend with an Arrhenius relation as shown in Fig. 5. From these fits, we obtained activation energies of $E_A = 66$ meV and 24 meV for PDI-C1 and PDI-C8, respectively. The different energies point out to the relevance of subtle changes in film packing on exciton dynamics. These values are of the same magnitude as those reported for strongly coupled chromophores.⁵ In the case of tetracene²² and

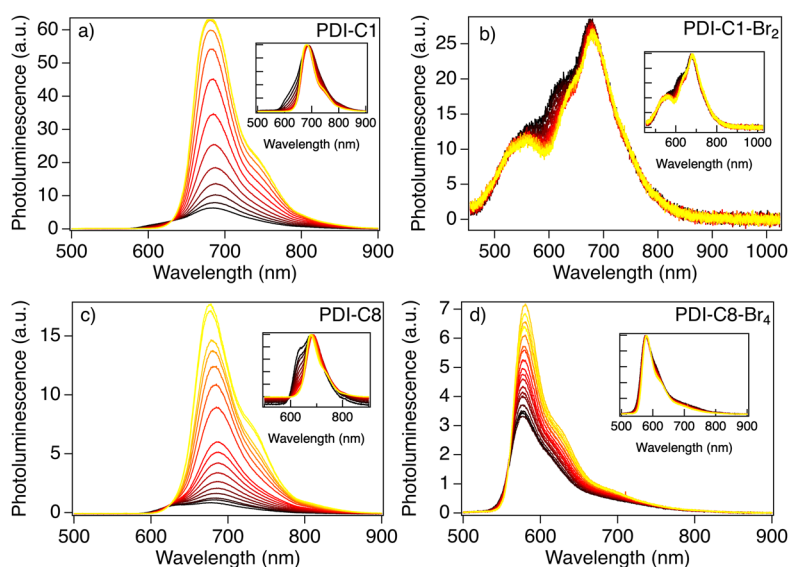


FIG. 4. Temperature dependent emission spectra measurements of thin films of PDI-C1 (a), PDI-C1-Br₂ (b), PDI-C8 (c), and PDI-C8-Br₄ (d) as measured in the home built helium cryostat setup. The temperatures vary from 13 K (yellow) to maximally 333 K (black). The insets show emission spectra normalized at the peak emission wavelength.

rubrene,²³ these activation energies have been attributed to thermally activated nonradiative recombination or singlet fission. However, as singlet fission in PDIs is known to occur on a sub-ps¹ to ps² time scale and the time resolution of our photoluminescence setup is 50 ps, it may be that SF is too fast to be responsible for the observed activation energy. Therefore, it is unlikely that the calculated activation energies for the PDIs belong to the thermally activated singlet fission process. Therefore, we have investigated the effects of other possible nonradiative decay pathways to determine a possible relationship between the observed thermally activated behavior and SF. First, thermal relaxation related to nonradiative losses has been considered. To that end, we studied the temperature dependence of the PL of isolated PDI molecules (in which SF cannot occur) using a solution of a hexylheptyl-imide substituted PDI in the glassy solvent 2Me-THF. The PL lifetime of the dissolved molecule remained unaffected by temperature as shown in Fig. S6 of the [supplementary material](#). This indicates that internal conversion and energy dissipation from the PDI to its surroundings are not responsible for the thermally activated decay process observed in the thin films. A second, more likely possibility is the formation of exothermic fluorescent excimers that are known to occur in closely packed PDIs.^{9,19,21} Excimer emission is strongly red shifted compared to fluorescence from isolated molecules which matches with the observations. Furthermore, the increased PL lifetimes at low temperatures for PDI-C1 and PDI-C8 point out to the formation of excimer states as the main contributor to the PDI photoluminescence and as such the found activation energies.

C. Transient absorption measurements on PDI films

While the thermally activated deactivation process is mainly related to the formation of excimers as argued above, PDIs are known to undergo SF with high efficiency in some cases. Therefore, we have performed femtosecond transient absorption (fs-TA) measurements on the thin films of the four model compounds considered here to establish whether triplets are formed. The results of these measurements are shown in Fig. 6. We observe a strong ground state bleach (GSB) at short times that is reminiscent of the ground-state absorption spectrum (indicated by dashed lines). Furthermore, all PDIs show an absorption feature above 600 nm, as will be discussed below. The triplet absorption in PDIs is known to occur in the same region as the GSB.²⁴ Such an induced absorption feature is exactly what we observe in the 520–550 nm region for PDI-C1, PDI-C1-Br₂, and PDI-C8 at times immediately after the excitation pulse. The assignment of this positive absorption feature to a triplet absorption is consistent with the long lifetime (>2.7 ns) of this feature as shown in Fig. 7.

From the kinetics of the induced absorption above 600 nm, we observe a full decay of singlet excited states within 3 ns. The overlapping TA features of triplet-triplet absorption and GSB at wavelengths shorter than 600 nm extend well beyond 3 ns. PDI-C8-Br₄ exhibits a distinctly different behavior as the triplet-triplet absorption feature around 580 nm develops on much longer time scales than observed for the other three compounds. A positive transient absorption feature arises after 6 ps and continues to grow up to

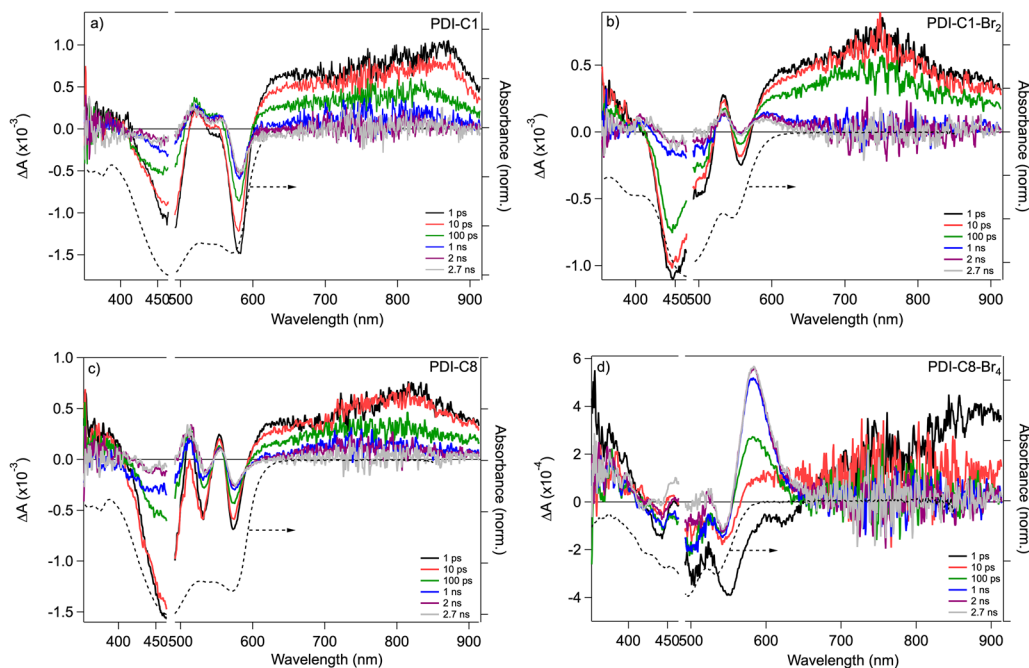


FIG. 6. Transient absorption spectra at different times of thin films of PDI-C1 (a), PDI-C1-Br₂ (b), PDI-C8 (c), and PDI-C8-Br₄ (d) on sapphire upon 480 nm excitation at 1.86×10^{12} (2.17×10^{13} for PDI-C8-Br₄) photons/cm². The dashed line indicates the normalized absorption spectrum of the respective PDI thin films.

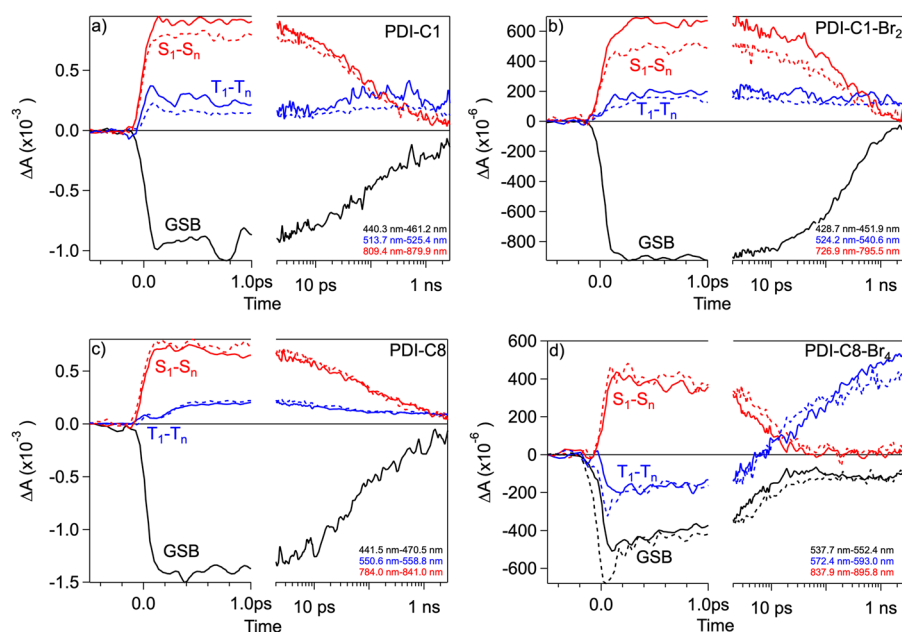


FIG. 7. Kinetic traces of the ground state bleach (GSB), triplet absorption (T_1-T_n), and the singlet absorption (S_1-S_n) for PDI-C1 (a), PDI-C1-Br₂ (b), PDI-C8 (c), and PDI-C8-Br₄ (d) on sapphire (solid lines) and fused silica (dashed lines) substrates. The traces are the average of a wavelength region as indicated in the lower right corner.

~ 1 ns. This long lived state cannot be due to thermal heating artefacts²⁵ since the triplet absorption for this molecule is red-shifted, away from the ground state absorption spectrum. Moreover, the existence of long lived triplet species in analogous tetra-brominated PDIs¹² substantiates the triplet origin of this long-lived feature. In fact, the DFT calculations on triplet spectra, provided in Table I, show that bromination leads to a red-shifted triplet absorption going from 2.31 eV (536 nm), to 2.19 eV (566 nm) and 2.14 eV (579 nm) for -Br₀, -Br₂, and -Br₄ substituted PDIs, respectively, which is similar to the triplet-triplet absorption maximum observed in TA. The rising triplet signal for PDI-C8-Br₄ was approximated with a monoexponential function and resulting in a singlet fission time of $\tau_{SF} = 16.2$ ps ($k_{SF} = 6.17 \times 10^{10} \text{ s}^{-1}$). To confirm the distinct behavior of PDI-C8-Br₄, we performed TA measurements on a similar tetrabrominated PDI, i.e., PDI-C1-Br₄. Very similar kinetics were obtained as for PDI-C8-Br₄, giving a characteristic time of $\tau_{SF} = 19.7$ ps ($k_{SF} = 5.08 \times 10^{10} \text{ s}^{-1}$), as shown in Fig. S7 of the supplementary material. As the SF rise time and overall excited state kinetics of PDI-C1-Br₄ and PDI-C8-Br₄ are very similar, it seems that bay-area bromination dominates the singlet fission behavior more than the imide substitution.

The photoinduced absorption above 600 nm is commonly attributed to the S_1-S_n transition in PDIs.² However, taking into account the temperature dependent PL measurements, it is likely that the photoinduced absorption 600–900 nm region is at least partly due to excimer states. This also explains why the decay of this absorption feature does not correlate with the rise of the T_1-T_n absorption in PDI-C1, PDI-C8, and PDI-C1-Br₂. This indicates that SF is not the only or even the primary decay process for the S_1 states. Considering the temperature dependent fluorescence measurements presented above, we conclude that SF competes with excimer formation at short times. This results in the formation of a limited fraction of triplets formed by SF while the remaining singlets

transform into excimer states. These excimers have a lower energy and are not sufficiently energetic to undergo SF.²⁶ A notable exception to this behavior is PDI-C8-Br₄ as the decay of the S_1-S_n matches the growth of the T_1-T_n absorption. This indicates that excimer formation is prohibited in PDI-C8-Br₄ by the strong twisting of the core. Therefore, the decay of the singlet population correlates with the growth of the triplets as there is no competing process here. The transient absorption measurements presented here indicate that a reduced excitonic interaction between neighboring molecules does not necessarily inhibit the occurrence of SF, but may be beneficial for SF because it prevents excimer formation. This shows that significant modifications to the PDI structure are possible leading to strongly enhanced solubility and reduced excitonic interactions while maintaining or even enhancing formation of triplet excited states.

The SF efficiency can be estimated via three main methods: (1) triplet sensitization to obtain a triplet extinction coefficient and subsequent subtraction from the spectrum, (2) global analysis using known extinction coefficients and spectra, and (3) the singlet depletion method, i.e., GSB quantization.²⁷ All methods have their weaknesses and are not regularly in agreement, which is why we have chosen not to calculate a triplet yield but describe the triplet feature qualitatively. For PDI-C1 and PDI-C8, we observe a strong triplet absorption feature that persists after 2.7 ns as was shown previously for PDI-C8.²⁵

In TA experiments, the pump fluences are typically high enough for singlet-singlet annihilation (SSA) to occur. The SSA leads to a hot singlet exciton that relaxes to the first excited singlet state while releasing energy as heat to the surroundings. This thermal heating of the surroundings is known to induce a temporal change in the absorption spectrum of the PDI and may lead to a thermal heating artefact in the GSB region of the TA spectrum.²⁵ To address the issue of SSA leading to a thermal heating artefact, we compared

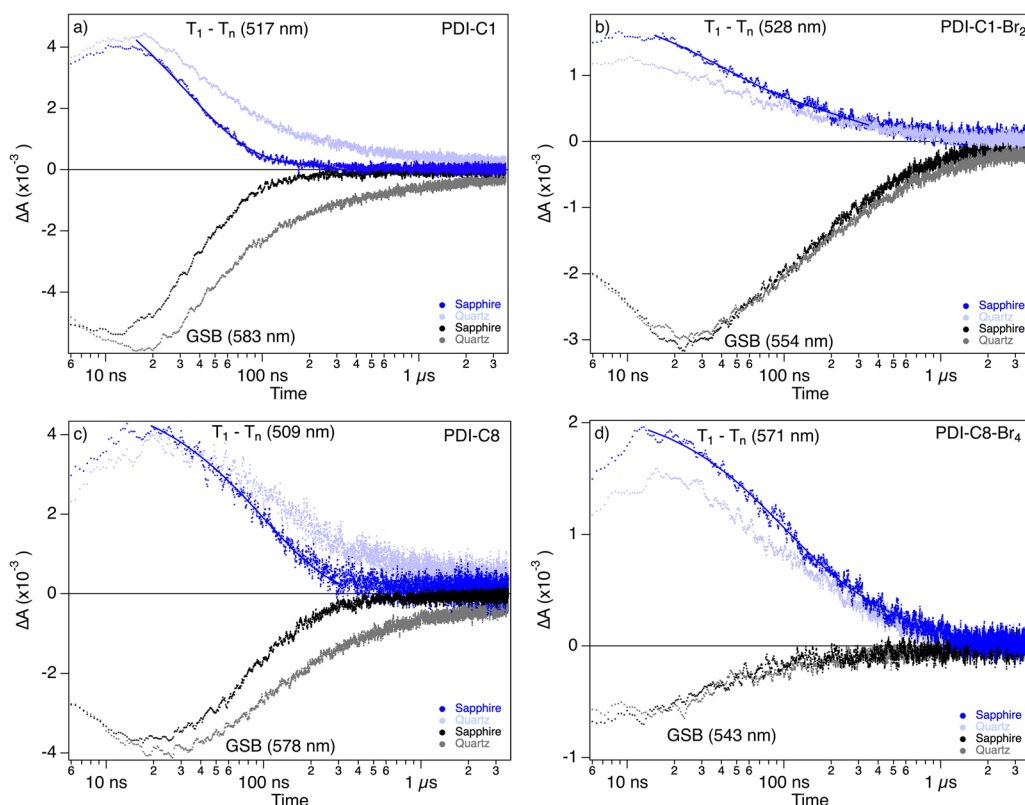


FIG. 8. Kinetic traces of GSB on sapphire (black) and fused silica or “quartz” (gray) and of the T_1-T_n on sapphire (blue) and quartz (light blue) substrates with thin films of PDI-C1 (a), PDI-C1-Br₂ (b), PDI-C8 (c), and PDI-C8-Br₄ (d) in the microsecond regime upon 480 nm excitation at a photon fluence of 2.10×10^{18} photons/cm².

the decay kinetics of T_1-T_n and S_1-S_n of the PDIs as a function of the substrate, i.e., fused silica (dashed line) and sapphire (solid line) glass, shown in Fig. 7. Since fused silica has an approximately 40 times lower thermal conductivity than sapphire, significant thermal heating artefacts due to SSA are expected, affecting both the absolute size and decay kinetics in the GSB region. As obvious from Fig. 7, the decay kinetics of singlet and triplet absorption is close to identical on fused silica and sapphire for PDI-C8 and PDI-C8-Br₄, while for PDI-C1 and PDI-C1-Br₂, the TA features in the sapphire film have a slightly larger magnitude. From this, we can conclude that the decay kinetics in PDIs at the used excitation fluence does not significantly affect the decay kinetics of the triplet as we should have seen an effect between fused silica and sapphire. The difference in absolute height may indicate a limited thermal heating effect, but the kinetics of the triplet absorption at 2.7 ns overlaps for both substrate-based samples making a triplet yield analysis via the singlet depletion method valid. To further study the effect of excitation fluence, we used an order of magnitude higher excitation fluence on the sapphire-based films, and in Fig. S8 of the [supplementary material](#), we observe a strong increase in the decay of all excited state species, indicative of SSA. This measurement shows how SSA can directly affect the excited state decay kinetics irrespective of thermal heating.

The lifetime of the triplet species generated by SF was studied using ns-TA experiments where we photoexcited the PDI samples on fused silica and sapphire at 480 nm (see Fig. 8). The ns-TA measurement shows a slower decay of the GSB and T_1-T_n of PDI-C1 and PDI-C8 in the case of a fused silica substrate, compared to sapphire which is in line with the dissipation of heat occurring after thermal heating of the sample (note that the excitation density in these experiments is much higher than in the fs-TA experiment). This clearly demonstrates the influence of SSA on the nano-to-microsecond excited state decay kinetics and the benefit of using sapphire

TABLE II. Triplet lifetimes as obtained from a biexponential fit on the ns-TA triplet transient.

PDI	T_1-T_n	
	$\tau_{T,1}$ (ns)	$\tau_{T,2}$ (ns)
C1	32.3 ± 0.5 (95%)	611.7 ± 313.0
C1-Br ₂	33.7 ± 2.0 (48%)	274.7 ± 10.4
C8	109.4 ± 1.0 (100%)	0
C8-Br ₄	83.4 ± 1.9 (60%)	482.3 ± 9.4

substrates at high fluences. For PDI-C1-Br₂, there is a weaker effect of the substrate, and thus thermal heating, on the observed decay kinetics of GSB and triplets and in PDI-C8-Br₄ there is hardly any difference between the two substrates which may either be due to the low optical density of the film or the fact that the triplet absorption is not overlapping with the GSB region for this compound. We can fit the triplet-triplet absorption with a biexponential decay and find a two-component triplet lifetime, provided in Table II, where the short component has a lifetime of $\tau_{T,1} = 30\text{--}80$ ns while the longer-lived component ranges from $\tau_{T,2} = 270\text{--}600$ ns. The existence of multiple triplet lifetimes may stem from the highly disordered nature of even polycrystalline solid-state systems where a variety of nonradiative decay processes may exist. This is consistent with the significantly lower triplet lifetime compared to that of PDIs in solution ($\tau_{T,s} > 30 \mu\text{s}$).²⁸ We also cannot rule out the effect due to triplet-triplet annihilation.

IV. CONCLUSION

In this work, we have examined the effect of bromination of the aromatic core of perylene diimide molecules on their excited state dynamics. We have measured the effect of bay-area bromination in PDIs on both the optical absorption, emission spectra and lifetime and found that bromination decreases the coupling and packing between PDI chromophores. Temperature dependent measurements show the presence of a temperature activated process, which is attributed to excimer formation. Ultrafast (fs) transient absorption measurements show that for all compounds, SF results in significant formation of triplet excited states, despite the pronounced changes in molecular packing on bromination. We conclude that in PDIs without bromines or only two bromines in the bay area, SF occurs in competition with excimer formation, resulting in relatively low SF yields. Introduction of four bromine atoms in the bay area results in significant distortion of the structure which prevents excimer formation. This shows that while bay area substitution of PDIs decreases the excitonic interactions between the neighboring molecules, this is in fact beneficial for SF as it prevents the occurrence of the competing process, i.e., excimer formation.

SUPPLEMENTARY MATERIAL

See [supplementary material](#) for a description of the synthesis and characterization of the new compounds presented, X-ray diffraction data of the samples, and supplementary temperature dependent absorption and emission data and additional data for a reference compound.

ACKNOWLEDGMENTS

This research leading to these results has received funding from the European Research Council Horizon 2020 ERC Grant Agreement No. 648433.

REFERENCES

- 1 Y. V. Aulin, K. M. Felner, D. Gunbas, R. K. Dubey, W. F. Jager, and F. Grozema, "Morphology independent efficient singlet exciton fission in perylenediimide thin films," *ChemPlusChem* **83**, 230–238 (2018).
- 2 S. W. Eaton, L. E. Shoer, S. D. Karlen, S. M. Dyar, E. A. Margulies, B. S. Veldkamp, C. Ramanan, D. A. Hartzler, S. Savikhin, and T. J. Marks, "Singlet exciton fission

in polycrystalline thin films of a slip-stacked perylenediimide," *J. Am. Chem. Soc.* **135**, 14701–14712 (2013).

- 3 A. K. Le, J. A. Bender, D. H. Arias, D. E. Cotton, J. C. Johnson, and S. T. Roberts, "Singlet fission involves an interplay between energetic driving force and electronic coupling in perylenediimide films," *J. Am. Chem. Soc.* **140**, 814–826 (2018).

- 4 T. N. Singh-Rachford, A. Nayak, M. L. Muro-Small, S. Goeb, M. J. Therien, and F. N. Castellano, "Supermolecular-chromophore-sensitized near-infrared-to-visible photon upconversion," *J. Am. Chem. Soc.* **132**, 14203–14211 (2010).

- 5 M. B. Smith and J. Michl, "Singlet fission," *Chem. Rev.* **110**, 6891–6936 (2010).

- 6 X. Feng, A. B. Kolomeisky, and A. I. Krylov, "Dissecting the effect of morphology on the rates of singlet fission: Insights from theory," *J. Phys. Chem. C* **118**, 19608–19617 (2014).

- 7 G. B. Piland and C. J. Bardeen, "How morphology affects singlet fission in crystalline tetracene," *J. Phys. Chem. Lett.* **6**, 1841–1846 (2015).

- 8 B. S. Basel, C. Hetzer, J. Zirzmeier, D. Thiel, R. Guldi, F. Hampel, A. Kahnt, T. Clark, D. M. Guldi, and R. R. Tykwinski, "Davydov splitting and singlet fission in excitonically coupled pentacene dimers," *Chem. Sci.* **10**, 3854–3863 (2019).

- 9 E. A. Margulies, C. E. Miller, Y. Wu, L. Ma, G. C. Schatz, R. M. Young, and M. R. Wasielewski, "Enabling singlet fission by controlling intramolecular charge transfer in Π -stacked covalent terrylenediimide dimers," *Nat. Chem.* **8**, 1120 (2016).

- 10 F. Mirjani, N. Renaud, N. Gorczak, and F. C. Grozema, "Theoretical investigation of singlet fission in molecular dimers: The role of charge transfer states and quantum interference," *J. Phys. Chem. C* **118**, 14192–14199 (2014).

- 11 N. Renaud and F. C. Grozema, "Intermolecular vibrational modes speed up singlet fission in perylenediimide crystals," *J. Phys. Chem. Lett.* **6**, 360–365 (2015).

- 12 K. Nagarajan, A. R. Mallia, V. S. Reddy, and M. Hariharan, "Access to triplet excited state in core-twisted perylenediimide," *J. Phys. Chem. C* **120**, 8443–8450 (2016).

- 13 E. Mete, D. Uner, M. Cakmak, O. Gulseren, and Ş. Ellialtıođlu, "Effect of molecular and electronic structure on the light-harvesting properties of dye sensitizers," *J. Phys. Chem. C* **111**, 7539–7547 (2007).

- 14 J. M. Duff, A.-M. Hor, A. R. Melnyk, and D. Teney, "Spectral response and xerographic electrical characteristics of some perylene bisimide pigments," in *Hard Copy and Printing Materials, Media, and Processes* (International Society for Optics and Photonics, 1990), pp. 183–192.

- 15 Z. B. Hill, D. B. Rodovsky, J. M. Leger, and G. P. Bartholomew, "Synthesis and utilization of perylene-based N-type small molecules in light-emitting electrochemical cells," *Chem. Commun.* **48**, 6594–6596 (2008).

- 16 S. Sengupta, R. K. Dubey, R. W. Hoek, S. P. van Eeden, D. D. Gunbaş, F. C. Grozema, E. J. Sudhölter, and W. F. Jager, "Synthesis of regioisomerically pure 1, 7-dibromoperylene-3, 4, 9, 10-tetracarboxylic acid derivatives," *J. Org. Chem.* **79**, 6655–6662 (2014).

- 17 Z. Chen, U. Baumeister, C. Tschierske, and F. Würthner, "Effect of core twisting on self-assembly and optical properties of perylene bisimide dyes in solution and columnar liquid crystalline phases," *Chem. - Eur. J.* **13**, 450–465 (2007).

- 18 F. Würthner, C. Thalacker, S. Diele, and C. Tschierske, "Fluorescent J-type aggregates and thermotropic columnar mesophases of perylene bisimide dyes," *Chem. - Eur. J.* **7**, 2245–2253 (2001).

- 19 C. Kaufmann, W. Kim, A. Nowak-Król, Y. Hong, D. Kim, and F. Würthner, "Ultrafast exciton delocalization, localization, and excimer formation dynamics in a highly defined perylene bisimide quadruple Π -stack," *J. Am. Chem. Soc.* **140**, 4253–4258 (2018).

- 20 E. A. Margulies, L. E. Shoer, S. W. Eaton, and M. R. Wasielewski, "Excimer formation in cofacial and slip-stacked perylene-3, 4: 9, 10-bis (dicarboximide) dimers on a redox-inactive triptycene scaffold," *Phys. Chem. Chem. Phys.* **16**, 23735–23742 (2014).

- 21 M. Son, K. H. Park, C. Shao, F. Würthner, and D. Kim, "Spectroscopic demonstration of exciton dynamics and excimer formation in a sterically controlled perylene bisimide dimer aggregate," *J. Phys. Chem. Lett.* **5**, 3601–3607 (2014).

- 22 J. Burdett, D. Gosztola, and C. J. Bardeen, "The dependence of singlet exciton relaxation on excitation density and temperature in polycrystalline tetracene thin films: Kinetic evidence for a dark intermediate state and implications for singlet fission," *J. Chem. Phys.* **135**, 214508 (2011).

- ²³J. Li, Z. Chen, Q. Zhang, Z. Xiong, and Y. Zhang, "Temperature-dependent singlet exciton fission observed in amorphous rubrene films," *Org. Electron.* **26**, 213–217 (2015).
- ²⁴W. E. Ford and P. V. Kamat, "Photochemistry of 3, 4, 9, 10-perylene-tetracarboxylic dianhydride dyes. 3. Singlet and triplet excited-state properties of the bis (2, 5-di-tert-butylphenyl) imide derivative," *J. Phys. Chem.* **91**, 6373–6380 (1987).
- ²⁵A. K. Le, J. A. Bender, and S. T. Roberts, "Slow singlet fission observed in a polycrystalline perylene diimide thin film," *J. Phys. Chem. Lett.* **7**, 4922–4928 (2016).
- ²⁶C. B. Dover, J. K. Gallaher, L. Frazer, P. C. Tapping, A. J. Petty II, M. J. Crossley, J. E. Anthony, T. W. Kee, and T. W. Schmidt, "Endothermic singlet fission is hindered by excimer formation," *Nat. Chem.* **10**, 305 (2018).
- ²⁷C. M. Mauck, P. E. Hartnett, E. A. Margulies, L. Ma, C. E. Miller, G. C. Schatz, T. J. Marks, and M. R. Wasielewski, "Singlet fission via an excimer-like intermediate in 3, 6-bis (thiophen-2-yl) diketopyrrolopyrrole derivatives," *J. Am. Chem. Soc.* **138**, 11749–11761 (2016).
- ²⁸Z. Yu, Y. Wu, Q. Peng, C. Sun, J. Chen, J. Yao, and H. Fu, "Accessing the triplet state in heavy-atom-free perylene diimides," *Chem. - Eur. J.* **22**, 4717–4722 (2016).